



OPEN ACCESS

## EXTENDED REPORT

Halofuginone attenuates osteoarthritis by inhibition of TGF- $\beta$  activity and H-type vessel formation in subchondral boneZhuang Cui,<sup>1,2</sup> Janet Crane,<sup>1</sup> Hui Xie,<sup>1</sup> Xin Jin,<sup>1</sup> Gehua Zhen,<sup>1</sup> Changjun Li,<sup>1</sup> Liang Xie,<sup>1</sup> Long Wang,<sup>1</sup> Qin Bian,<sup>1</sup> Tao Qiu,<sup>1</sup> Mei Wan,<sup>1</sup> Min Xie,<sup>3</sup> Sheng Ding,<sup>3</sup> Bin Yu,<sup>2</sup> Xu Cao<sup>1</sup>**Handling editor** Tore K Kvien

► Additional material is published online only. To view, please visit the journal online (<http://dx.doi.org/10.1136/annrheumdis-2015-207923>).

<sup>1</sup>Department of Orthopaedic Surgery, Institute for Cell Engineering, Johns Hopkins University, Baltimore, Maryland, USA

<sup>2</sup>Department of Orthopaedics and Traumatology, Nanfang Hospital, Southern Medical University, Guangzhou, Guangdong, China

<sup>3</sup>Department of Pharmaceutical Chemistry, Gladstone Institute of Cardiovascular Disease, University of California, San Francisco, California, USA

**Correspondence to**

Professor Xu Cao, Department of Orthopaedic Surgery, Institute for Cell Engineering, Johns Hopkins University, Baltimore, MD 21205, USA; [xcao11@jhmi.edu](mailto:xcao11@jhmi.edu) and Bin Yu; [yubinol@163.com](mailto:yubinol@163.com)

Received 14 May 2015

Revised 1 September 2015

Accepted 20 September 2015

Published Online First

15 October 2015

**ABSTRACT**

**Objectives** Examine whether osteoarthritis (OA) progression can be delayed by halofuginone in anterior cruciate ligament transection (ACL) rodent models.

**Methods** 3-month-old male C57BL/6J (wild type; WT) mice and Lewis rats were randomised to sham-operated, ACLT-operated, treated with vehicle, or ACLT-operated, treated with halofuginone. Articular cartilage degeneration was graded using the Osteoarthritis Research Society International (OARSI)-modified Mankin criteria. Immunostaining, flow cytometry, RT-PCR and western blot analyses were conducted to detect relative protein and RNA expression. Bone micro CT ( $\mu$ CT) and CT-based microangiography were quantitated to detect alterations of microarchitecture and vasculature in tibial subchondral bone.

**Results** Halofuginone attenuated articular cartilage degeneration and subchondral bone deterioration, resulting in substantially lower OARSI scores. Specifically, we found that proteoglycan loss and calcification of articular cartilage were significantly decreased in halofuginone-treated ACLT rodents compared with vehicle-treated ACLT controls. Halofuginone reduced collagen X (Col X), matrix metalloproteinase-13 and A disintegrin and metalloproteinase with thrombospondin motifs 5 (ADAMTS 5) and increased lubricin, collagen II and aggrecan. In parallel, halofuginone-attenuated uncoupled subchondral bone remodelling as defined by reduced subchondral bone tissue volume, lower trabecular pattern factor (Tb.pf) and increased thickness of subchondral bone plate compared with vehicle-treated ACLT controls. We found that halofuginone exerted protective effects in part by suppressing Th17-induced osteoclastic bone resorption, inhibiting Smad2/3-dependent TGF- $\beta$  signalling to restore coupled bone remodelling and attenuating excessive angiogenesis in subchondral bone.

**Conclusions** Halofuginone attenuates OA progression by inhibition of subchondral bone TGF- $\beta$  activity and aberrant angiogenesis as a potential preventive therapy for OA.

**INTRODUCTION**

Osteoarthritis (OA), characterised by articular cartilage degeneration, joint pain and functional impairment, affects nearly 27 million people in the USA alone.<sup>1–2</sup> There is no effective disease-modifying treatment for OA until the end stage of disease necessitating joint replacement.<sup>3–4</sup> Despite

the identified risk factors, for example, mechanical, metabolic or genetic, the exact pathogenesis of OA is still unclear<sup>5</sup> and remains an active area of investigation as targets for preventive and disease-modifying therapies are greatly needed.

The aetiology of OA is multifactorial and includes intrinsic and extrinsic factors that propagate a multitude of cellular responses.<sup>6</sup> The resultant phenotype includes articular cartilage degeneration, subchondral bone sclerosis and oedema, osteochondral angiogenesis, inflammation and osteophyte formation.<sup>6–8</sup> Changes in the subchondral bone microarchitecture have been described to precede articular cartilage damage in OA.<sup>9–13</sup> Articular cartilage and subchondral bone form a functional unit in the joint.<sup>14–15</sup> Articular cartilage acts as a bearing, while subchondral bone acts as a structural girder and shock absorber.<sup>16</sup> Subchondral bone, separated by the cement line from the calcified zone of the articular cartilage, consists of the subchondral bone plate (SBP) and the subarticular spongiosa.<sup>17</sup> The architecture of subchondral bone and plate adapt via modelling and remodelling in response to mechanical stress.<sup>8–17</sup> Coupled bone remodelling ensures the integrity of the subchondral bone, where osteoclast and osteoblast activity are temporally and spatially regulated. Specifically, osteoclasts resorb bone and generate a bone marrow microenvironment that coordinates the migration and differentiation of cells to support angiogenesis and osteogenesis for subsequent osteoblast bone formation.<sup>18–21</sup>

Following an acute injury, such as anterior cruciate ligament tear, osteoclast bone resorption dramatically increases.<sup>22–24</sup> The subchondral bone marrow microenvironment changes substantially and results in woven bone and angiogenesis. We have previously found that excessive activation of TGF- $\beta$ 1 by elevated osteoclast bone resorption uncouples bone resorption and formation, contributing to the sclerotic phenotype in the subchondral bone in OA animal models.<sup>18–25</sup> Specifically, high levels of TGF- $\beta$  result in erroneous recruitment of mesenchymal/stromal stem cells (MSCs) and formation of osteoid islets. The progression of OA could be attenuated, but not completely abrogated, by inhibiting TGF- $\beta$ 1 signalling.<sup>26</sup> Vascularisation and innervation of articular cartilage have also been noted in OA, with blood vessels and nerves originating from subchondral bone and breaching the



CrossMark

**To cite:** Cui Z, Crane J, Xie H, et al. *Ann Rheum Dis* 2016;**75**:1714–1721.

tide mark in the early stages.<sup>27 28</sup> A specific subtype of vessels, termed H-type vessels and defined by high costaining for CD31 and endomucin (CD31<sup>hi</sup>Emcn<sup>hi</sup>), has been identified to couple angiogenesis and osteogenesis.<sup>20 29</sup> A therapy that is able to target the multiple pathological changes in subchondral bone would be desired.

The small molecule halofuginone (HF) is an analogue of febrifugine, which was isolated from the plant *Dichroa febrifuga* in ancient Chinese herbal medicine for the treatment of malarial fever.<sup>30 31</sup> HF has shown therapeutic promise in clinical trials for fibrotic diseases, such as scleroderma and chronic graft-versus-host disease by inhibiting phosphorylation of Smad2/3 and TGF- $\beta$ -mediated collagen type I synthesis.<sup>32 33</sup> HF has also been reported to inhibit the differentiation of the CD4 + T helper cell subset, Th17,<sup>34</sup> elucidating beneficial effects in an autoimmune arthritis mouse model.<sup>35</sup> Th17 functions as an osteoclastogenic CD4+ helper T cell subset that links T cell activation and bone destruction.<sup>36 37</sup> Th17 cells produce interleukin (IL) 17, inducing the expression of receptor activator of nuclear factor  $\kappa$  B ligand (RANKL) to promote osteoclastogenesis.<sup>38 39</sup> TGF- $\beta$  is essential for the initiation of Th17 differentiation.<sup>40 41</sup> HF has also been shown to induce antiangiogenic effects in preclinical studies at several essential stages of angiogenesis, largely through inhibition of matrix metalloproteinase-2 (MMP-2).<sup>42</sup> As increased CD4+ T cell subsets, high TGF- $\beta$  concentrations and angiogenesis have been shown to be involved in the pathogenesis of OA,<sup>43 44</sup> we investigated the potential effect of HF as a preventive treatment for OA. We found that HF could attenuate progression of OA by delaying articular cartilage degeneration and subchondral bone sclerosis in rodent anterior cruciate ligament transection (ACLT) models by inhibiting Th17

differentiation, TGF- $\beta$ -dependent Smad2/3 phosphorylation and angiogenesis.

## MATERIALS AND METHODS

Three-month-old male C57BL/6J (WT) mice and Lewis rats were purchased from Charles River. Rodents were randomised to sham-operated, ACLT-operated, treated with vehicle or ACLT-operated, treated with HF. We performed histological analysis using Safranin O-fast green and H&E staining and graded articular cartilage degeneration using the Osteoarthritis Research Society International (OARSI)-modified Mankin criteria.<sup>45</sup> Immunostaining, flow cytometry, RT-PCR and western blot analyses were conducted to detect relative protein expression. We quantitated bone micro CT ( $\mu$ CT) and CT-based microangiography parameters to detect the alterations of microarchitecture and vasculature in tibial subchondral bone. A detailed description of the Material and methods can be found in the online supplementary text.

## RESULTS

### HF attenuates progression of OA in ACLT mice

To investigate the effects of HF on disease activity and progression in OA, we administered HF intraperitoneally in mice after ACLT. The optimal dose (1 mg/kg body weight (mg/kg)) was identified using multiple concentrations of HF (0.2, 0.5, 1 or 2.5 mg/kg) injected every other day for 1 month post surgery (see online supplementary figure S1). Lower concentration (0.2 or 0.5 mg/kg) had minimal effects on subchondral bone and higher concentration (2.5 mg/kg) induced proteoglycan loss in articular cartilage. Specifically, Safranin O staining demonstrated retention of proteoglycan and decreased thickness of calcified

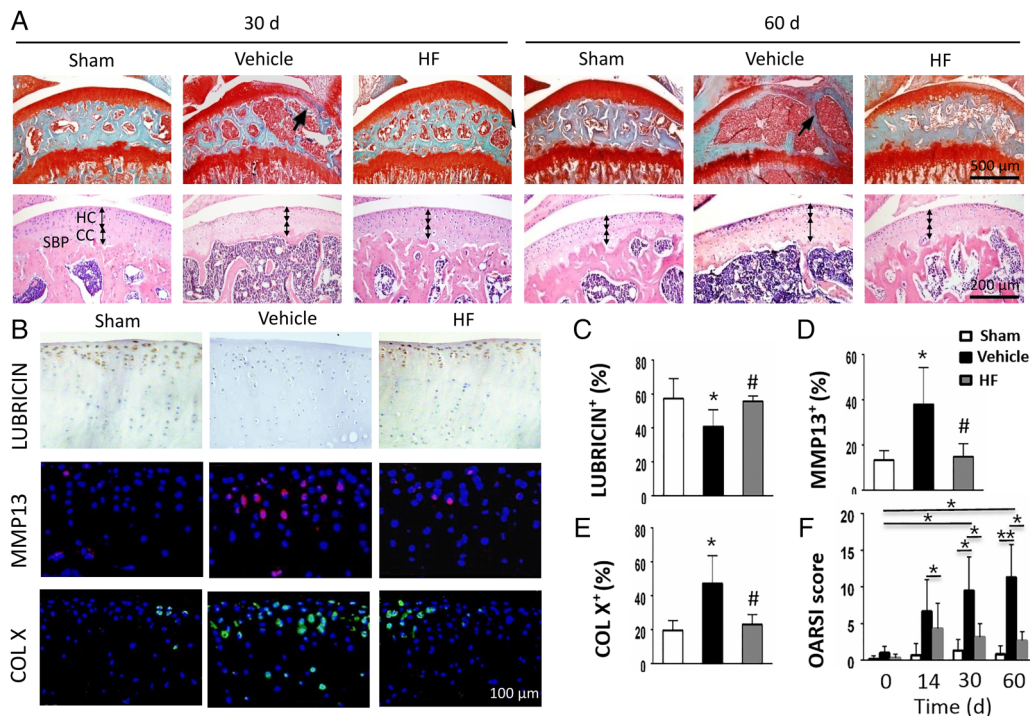


**Figure 1** Halofuginone preserves articular cartilage after anterior cruciate ligament transection (ACLT). (A) Safranin O and fast green staining (top). Solid arrows indicate proteoglycan loss and cartilage destruction at 30 and 60 days post operation. Scale bar, 500  $\mu$ m. H&E staining (bottom) where calcified cartilage (CC) and hyaline cartilage (HC) thickness are marked by double-headed arrows. Scale bars, 200  $\mu$ m. (B–E) Immunostaining and quantitative analysis of lubricin (B-top, C), matrix metalloproteinase (MMP) 13 (B-middle, D) and COL X (B-bottom, E) in articular cartilage at 30 days post operation. Scale bar, 100  $\mu$ m. (F) Osteoarthritis Research Society International–modified Mankin scores of articular cartilage at 0, 14, 30 and 60 days after surgery. Sham=sham-surgery. Vehicle=ACLT-surgery treated with vehicle. HF=ACLT-surgery treated with halofuginone. n=6 per group. \*p<0.05 compared with sham or as denoted by bar, \*\*<0.01 compared as denoted by bar; #p<0.05 compared with the vehicle.

**Table 1** Cartilage thickness changes in different group and time-points (10× magnified images; mean±SD; unit: mm)

Time (days)	HC			CC		
	Sham	Vehicle	Halofuginone	Sham	Vehicle	Halofuginone
14	0.83±0.028	0.79±0.046	0.81±0.041	0.32±0.032	0.3±0.028	0.28±0.037
30	0.81±0.028	0.77±0.053	0.81±0.023	0.33±0.031	0.34±0.052	0.28±0.014
60	0.77±0.175	0.45±0.18*	0.76±0.112 <sup>†</sup>	0.32±0.186	0.65±0.19*	0.35±0.113 <sup>†</sup>

The level of significance was set at  $p < 0.05$  and indicated by ‘\*\*’ for the comparison between vehicle-treated group and sham group, or ‘†’ for the comparison between halofuginone-treated group and vehicle-treated group. CC, calcified cartilage; HC, hyaline cartilage.

cartilage zone (from the tidemark line to SBP) in HF-treated ACLT mice (1 mg/kg) relative to vehicle-treated ACLT controls (figure 1A and table 1). HF normalised expression of lubricin, MMP-13 and collagen X (Col X), collagen II, aggrecan and A disintegrin and metalloproteinase with thrombospondin motifs 5 (ADAMTS 5) as assessed by immunostaining and RT-PCR in the HF-treated ACLT mice relative to sham controls (figure 1B–E and online supplementary figures S2 and S3). OARSI scores were improved in HF-treated ACLT mice relative to vehicle-treated ACLT controls, whereas no difference was noted in HF versus sham controls (figure 1F).

**HF sustains coupled subchondral bone remodelling**

The effect of HF on the structure of tibial subchondral bone was analysed by  $\mu$ CT. HF significantly reduced the tibial subchondral bone tissue volume (TV), lowered trabecular pattern

factor (Tb.pf) and increased SBP thickness post ACLT relative to vehicle treatment (figure 2A–D). There was no statistically significant difference in TV, Tb.pf or SBP thickness between the HF-treated ACLT mice and sham controls. Consistently, the number of tartrate-resistant acid phosphatase-positive osteoclast cells and osteoprogenitor osterix-positive cells increased after ACLT (vehicle vs sham) (figure 2E–H). The increase in both cell populations was abrogated by HF treatment (figure 2E–H). Notably, in the vehicle-treated ACLT mice, the majority of osterix-positive cells were found in clusters in subchondral bone marrow compared with localisation predominately on the bone surface in the HF-treated ACLT mice (figure 2G,H).

We also examined the effect of local administration of HF on OA progression in ACLT rats by embedding HF containing alginate beads directly into the tibial subchondral bone. Similar to administration of TGF- $\beta$  neutralising antibody (1D11) in the

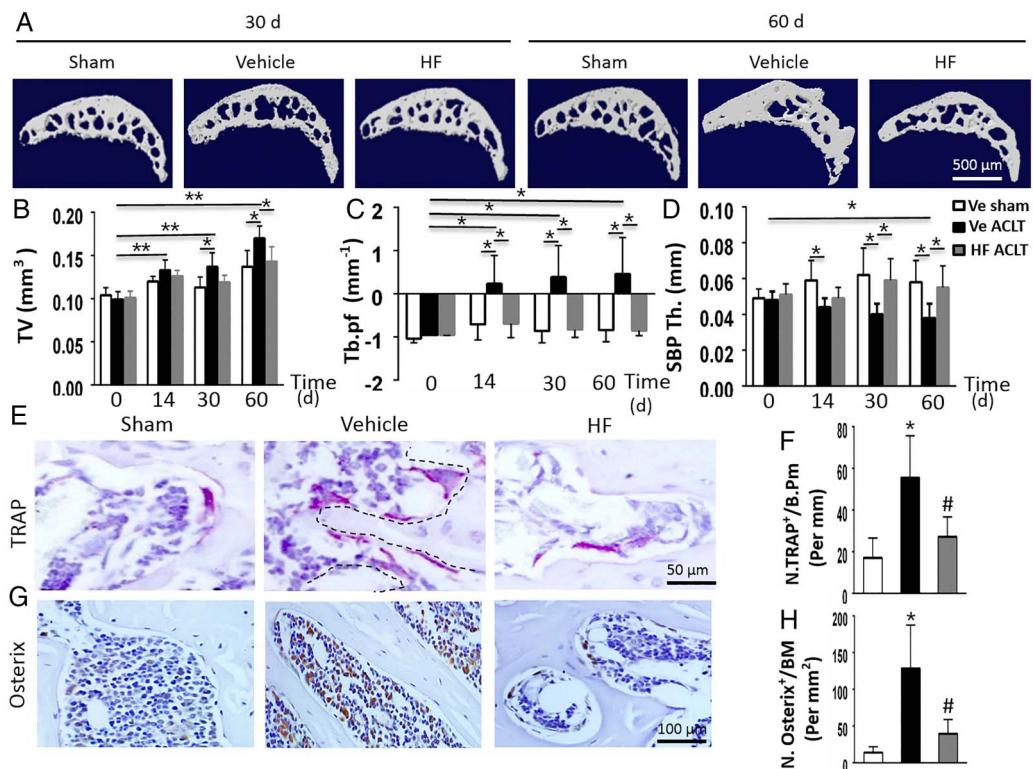


**Figure 2** Halofuginone normalises subchondral bone after anterior cruciate ligament transection (ACLT). (A) Representative three dimensional micro-CT images of sagittal views of subchondral bone medial compartment at 30 and 60 days after sham operation or ACLT surgery. Scale bar, 500  $\mu$ m. (B–D) Quantitative micro-CT analysis of tibial subchondral bone of total tissue volume (TV) (B), trabecular pattern factor (Tb.pf) (C) and subchondral bone plate thickness (D). (E and F) Tartrate-resistant acid phosphatase (TRAP) staining (E) and quantitative analysis (F) at 14 days after surgery. Scale bar, 50  $\mu$ m. (G and H) Immunohistochemical staining (G) and quantification (H) of osterix-positive cells (brown) in subchondral bone 30 days after surgery. Scale bar, 100  $\mu$ m. Sham=sham-surgery. Vehicle=ACLT-surgery treated with vehicle. HF=ACLT-surgery treated with halofuginone. n=6 per group. \* $p < 0.05$  compared with sham or as denoted by bar, \*\* $p < 0.01$  compared as denoted by bar; # $p < 0.05$  compared with the vehicle.

subchondral bone rats, articular cartilage was protected in the HF-treated rats as demonstrated by retention of proteoglycan, MMP-13 and Col X staining (see online supplementary figures S4A and S5). The subchondral bone microarchitecture was preserved with both 1D11 and HF treatments. Specifically, in the ACLT rats treated with vehicle, Tb.pf and TV were increased, while connectivity density and SBP Th. were decreased compared with sham control rats. ACLT rats treated with either HF or 1D11 did not show any statistically significant difference in these parameters relative to the sham control rats (see online supplementary figure S4A–E).<sup>26</sup>

### HF suppresses osteoclastogenesis by decrease of Th17 cells in the subchondral bone of mice

We examined whether HF inhibits osteoclastogenesis through modulation of Th17 cells. Immunofluorescence staining of Th17 specific markers (CD4 and IL17) revealed a significant increase of Th17 cells in the subchondral bone marrow of vehicle-treated mice as early as 2 weeks post surgery, whereas HF-treated mice had equivalent Th17 cells compared with sham controls (figure 3A,B). Consistently, a significant increase of Th17 cells (CD4+IL17+) in the bone marrow 14 days post surgery in vehicle-treated mice was also observed using flow cytometry analysis. HF-treated ACLT mice had significantly decreased Th17 cells, similar to the level of sham controls (figure 3C,D). The number of CD4<sup>+</sup>IL17<sup>+</sup> cells in bone marrow and peripheral blood remained unchanged at different time-points (see online supplementary figure S6). Changes in bone marrow Th17 cell numbers were time-dependent, with

Th17 cell numbers decreasing to baseline (0 day) in the ACLT-vehicle treated mice 2 months post surgery (see online supplementary figure S7A–C). No difference in the number of Th17 cells in peripheral blood was noted regardless of vehicle or HF-treated mice relative to sham controls (figure 3C,D).

In parallel with the increased aggregation of Th17 cells in the subchondral bone marrow of vehicle-treated mice, an increase in expression of RANKL was observed in the subchondral bone compared with sham controls (figure 3E,F). HF treatment significantly attenuated RANKL expression with no significant difference noted relative to sham controls (figure 3E,F). The results indicate HF inhibits osteoclastogenesis by decreasing Th17 cells and RANKL expression in the subchondral bone.

### HF inhibits Smad2/3-dependent TGF- $\beta$ signalling pathway in bone marrow MSCs

Immunofluorescence staining of nestin showed that HF significantly attenuated the increase in number of MSCs in the subchondral bone post ACLT relative to vehicle (figure 4A,B). There was no statistical difference between the number of nestin-positive cells in HF-treated ACLT mice relative to sham controls (figure 4A,B). Furthermore, nestin-positive cells were dispersed throughout the bone marrow in vehicle-treated mice compared with the closer proximity to the bone surface in the HF-treated mice (figure 4A). As high active TGF- $\beta$  recruits MSCs in the subchondral bone marrow, we investigated whether HF could directly inhibit TGF- $\beta$  signalling in MSCs. Western blot analysis of MSCs revealed that phosphorylation of Smad2 (pSmad2) was inhibited by HF in both a time-dependent and dose-

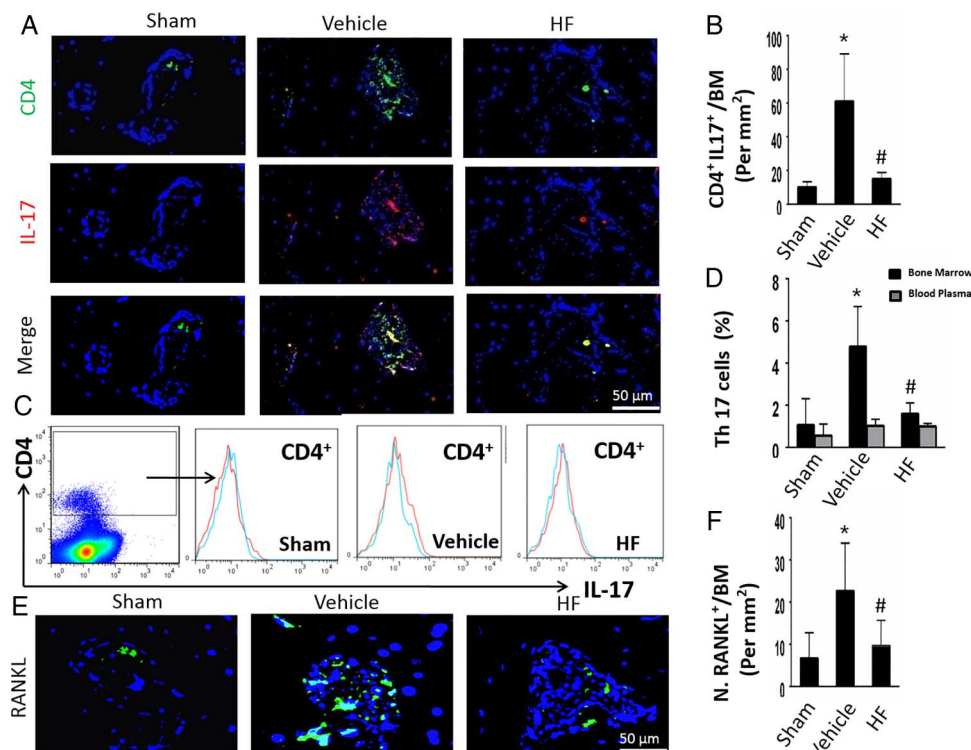


**Figure 3** Halofuginone suppresses Th17 cells after anterior cruciate ligament transection (ACLT). (A) Representative immunofluorescence double staining for CD4 (green), interleukin (IL) 17 (red) and merged images (colocalisation=yellow) 14 days after surgery. Scale bar, 50  $\mu$ m. (B) Quantitative analysis of the number of CD4+IL17+ (Th17) cells per bone marrow (BM) area ( $\text{mm}^2$ ). (C) Flow cytometry analysis of double staining Th17 (CD4+IL17+) cells in subchondral BM 14 days post surgery. The green line represents CD4+ cells in an unstained control. (D) Flow cytometry quantitative analysis of the percentage of Th17 cell in subchondral BM and peripheral blood plasma 14 days after surgery. (E and F) Immunofluorescence staining (E) and quantification (F) for receptor activator of nuclear factor  $\kappa$  B ligand (RANKL) in subchondral bone 14 days post surgery. Sham=sham-surgery. Vehicle=ACLT-surgery treated with vehicle. HF=ACLT-surgery treated with halofuginone. n=6 per group. \* $p$ <0.05, compared with the sham; # $p$ <0.05 compared with the vehicle.

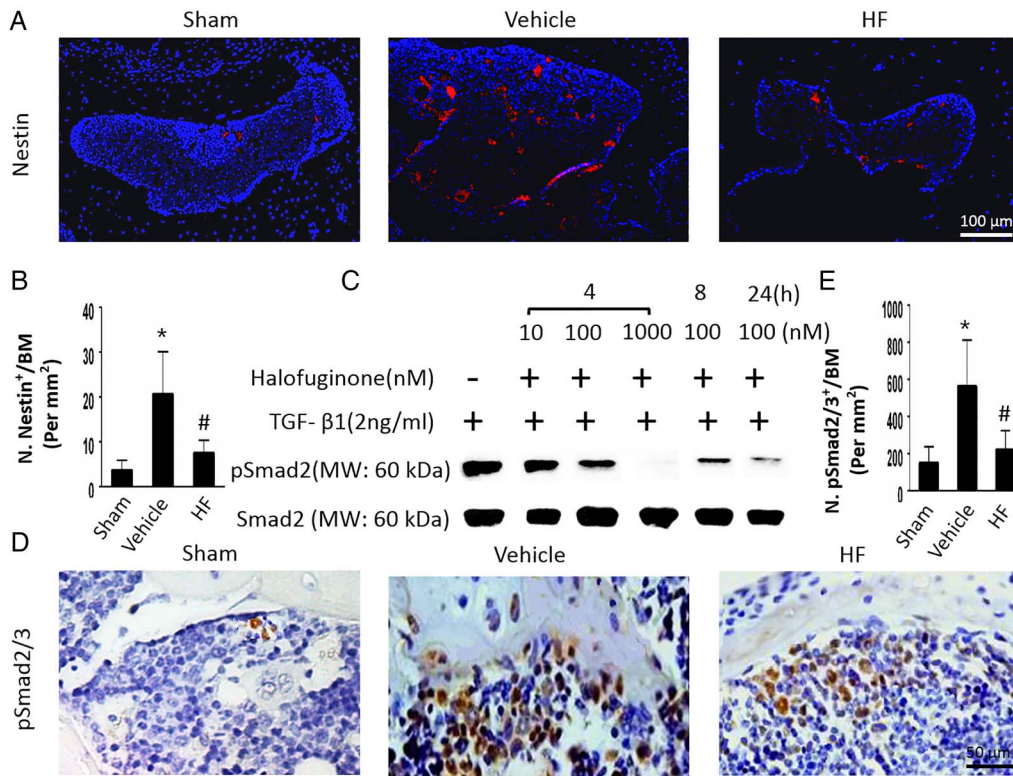


**Figure 4** Halofuginone restores coupled bone remodelling after anterior cruciate ligament transection (ACLT). (A) Immunofluorescence staining for nestin in sagittal sections of subchondral bone medial compartment 30 days post surgery. Scale bar, 100  $\mu$ m. (B) Quantitative analysis of the number of nestin-positive cells per bone marrow (BM) area of tibial subchondral bone. (C) Western blot analysis of the phosphorylation of Smad2 in cultured mesenchymal/stromal stem cells treated with the combination of recombinant human TGF- $\beta$ 1 and increasing doses of halofuginone after 4, 8 or 24 h. (D and E) Immunohistochemistry staining (D) and quantification (E) of pSmad2/3-positive cells in sagittal sections of subchondral bone medial compartment 14 days post surgery. Sham=sham-surgery. Vehicle=ACLT-surgery treated with vehicle. HF=ACLT-surgery treated with halofuginone. n=6 per group. Scale bar, 50  $\mu$ m. \*p<0.05 compared with the sham and #p<0.05 compared with the vehicle.

dependent manner (figure 4C). Immunohistochemistry staining of pSmad2/3 further validated HF inhibition of TGF- $\beta$  signalling in subchondral bone cells. Specifically, pSmad2/3-positive cells in the subchondral bone of vehicle-treated ACLT mice were significantly increased and attenuated with HF to levels comparable with sham mice (figure 4D,E).

#### HF abrogates aberrant blood vessel formation in subchondral bone

Finally, we examined the potential effects of HF on subchondral bone angiogenesis. Using CT-based angiography in microphil perfusion, we found the number and volume of blood vessels were significantly increased in the subchondral bone of vehicle-treated ACLT mice. HF inhibited the increase of vessel number and volume in subchondral bone relative to vehicle treatment, retaining vessel number and volume similar to sham controls (figure 5A–C). We further analysed the type of vessels inhibited by HF by performing double immunofluorescence staining for CD31 and endomucin, recently described as H-type vessels.<sup>29</sup> CD31<sup>hi</sup>Emcn<sup>hi</sup> blood vessels were significantly increased in the subchondral bone of vehicle-treated ACLT mice. HF restored CD31<sup>hi</sup>Emcn<sup>hi</sup> blood vessels similar to sham controls (figure 5D,F). Changes in H-type vessels correlated with a similar pattern in endothelial cell proliferation as evaluated by immunostaining and quantification of the number of endomucin-positive cells that costained positive for Ki67 (figure 5E,G). Additionally, MMP-2 levels were statistically increased in vehicle-treated ACLT mice, whereas the HF-treated ACLT mice

had similar MMP-2 levels compared with sham controls (figure 5H and online supplementary figure S8).

#### DISCUSSION

We have shown that HF preserves the subchondral bone microarchitecture to prevent articular cartilage degeneration by inhibition of Th17-induced osteoclastogenesis, excessive TGF- $\beta$  activity and H-type vessel formation in recruitment of MSCs for aberrant bone formation. Particularly, the protection of articular cartilage by local administration of HF in the subchondral bone post ACLT in rats further suggests that maintaining the microstructural integrity of subchondral bone provides an essential physiological environment for articular cartilage. Subchondral bone undergoes remodelling in response to changes in the mechanical loading environment, such as after ACLT.<sup>8</sup> Biochemical and biomechanical interplay between subchondral bone and articular cartilage mediates effects on articular cartilage.<sup>14</sup>

CD4<sup>+</sup> T cell subsets are infiltrated and involved in the pathogenesis of OA,<sup>43–44</sup> including Th17 cells.<sup>36–37</sup> Th17 cells produce IL-17, which, in bone, induces the expression of RANKL from osteoclastogenesis-supporting mesenchymal cells to promote osteoclastogenesis.<sup>38–39</sup> Therefore, Th17 can be regarded as an osteoclastogenic helper cell, linking T cell activation with bone destruction.<sup>39</sup> We observed, during OA development, a significant increase of Th17 cells in the subchondral bone marrow of vehicle-treated mice as early as 2 weeks post surgery by immunofluorescence staining and flow cytometry,

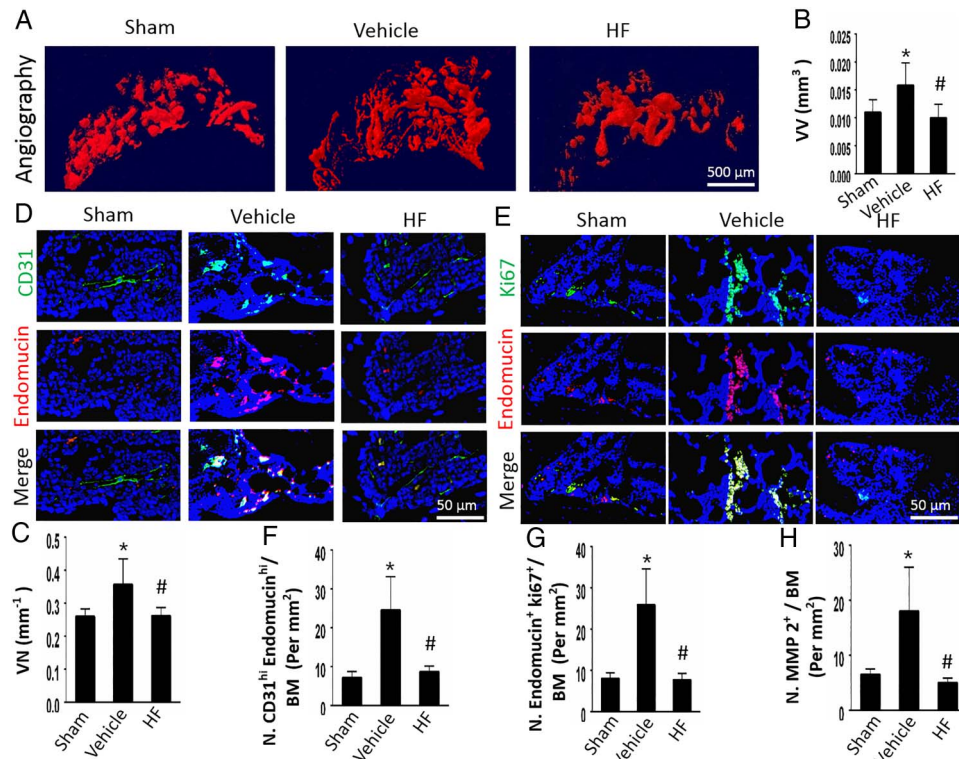


**Figure 5** Halofuginone attenuates aberrant angiogenesis in subchondral bone of anterior cruciate ligament transection (ACLT) mice. (A–C) Three dimensional CT-based microangiography of medial tibial subchondral bone (A) 30 days post surgery, with a quantification of vessel volume relative to tissue volume (VV/TV) (B) and vessel number (VN) (C). Scale bar, 500  $\mu$ m. (D and F) Representative immunofluorescence double staining (D) and quantification (F) of CD31 (green) and endomucin (red) positive cells 1 month after surgery. Scale bar, 50  $\mu$ m. (E and G) Immunofluorescence double staining (E) and quantification (G) of Ki67 (green) and endomucin (red) positive cells 1 month after surgery. Scale bar, 50  $\mu$ m. (H) Quantification of MMP-2 positive cells in subchondral bone marrow (BM) 1 month post surgery. Sham=sham-surgery. Vehicle=ACLT-surgery treated with vehicle. HF=ACLT-surgery treated with halofuginone. n=6 per group. \*p<0.05 compared with sham and #p<0.05 compared with vehicle.

with no significant changes in peripheral blood. We found the increase of Th17 cells in bone marrow was time-dependent, with Th17 cells numbers decreasing by 1 month and returning almost to baseline (0 day) by 2 months post surgery. We observed significantly increased expression of RANKL in the bone marrow in a similar time distribution. These results support that Th17 cells are involved in the onset of OA by promoting osteoclast bone resorption. The increase of Th17 cells (CD4+IL17+) and RANKL expression in bone marrow was inhibited by HF, indicating that HF inhibited osteoclastogenesis. HF is known to inhibit Th17 differentiation via inhibition of TGF- $\beta$  signalling and activating the amino acid response pathway.<sup>34</sup> TGF- $\beta$  can directly and indirectly initiate Th17 differentiation.<sup>40–41</sup> In intestinal cells, TGF- $\beta$  has been shown to increase expression of Runx1, which is necessary for Th17 differentiation.<sup>46</sup> TGF- $\beta$  can also block the signalling pathways that promote Th1 and Th2 differentiation,<sup>47–48</sup> thereby defaulting CD4+ T cell subsets to differentiate into the Th17 subtype. HF can also inhibit Th17 differentiation via activating the amino acid response pathway by suppressing prolyl-transfer RNA synthetase (ProRS) to induce uncharged tRNA accumulation within cells.<sup>49</sup> HF directly binds onto two different binding sites of ProRS via an ATP-dependent mechanism.<sup>50</sup>

Abnormal TGF- $\beta$  signalling-induced uncoupled subchondral bone remodelling precedes articular cartilage degeneration in ACLT OA mice.<sup>26</sup> HF likely maintains coupled bone remodelling through modulation of TGF- $\beta$  activity. During coupled bone remodelling, TGF- $\beta$  is released and activated during osteoclast bone resorption.<sup>25–51</sup> Smad2/3-dependent TGF- $\beta$  signalling

pathway induces migration of MSCs from their perivascular niche to the bone surface for osteoblast differentiation.<sup>25</sup> However, during OA development, excessive release and activation of TGF- $\beta$  will interrupt coupled bone remodelling, recruiting MSCs to form aberrant osteoid islets in bone marrow as opposed to bone resorption pits for coupled bone resorption. We found in vehicle-treated ACLT mice that the number of nestin-positive MSCs increased and clustered in bone marrow, indicating uncoupled bone remodelling. HF reduced MSCs numbers and relocated osterix-positive osteoprogenitors from the bone marrow to bone surface, re-establishing coupled bone remodelling. We speculate a combination of two mechanisms elicit this effect. The reduction in osteoclast bone resorption by HF likely reduces TGF- $\beta$  release from bone matrix. Additionally, both in vitro and in vivo evidences revealed that HF directly inhibits phosphorylation of Smad2 (pSmad2) in MSCs in both a time-dependent and dose-dependent manner, and likely prevents excessive MSC migration. These results, in combination with our previous findings, suggest that HF inhibits the formation of osteoid islets by suppressing TGF- $\beta$  signalling.<sup>26</sup>

Abnormal vascular congestion in subchondral bone is a known pathological feature of OA.<sup>52</sup> OA is thought to progress by osteochondral angiogenesis where blood vessels breach the tidemark at the osteochondral junction.<sup>53–54</sup> HF inhibits angiogenesis through indirectly inhibiting MMP-2-dependent tubular network formation.<sup>42</sup> MMP-2 can degrade structural extracellular matrix by cleaving type IV collagen,<sup>55–56</sup> the protein backbone of the endothelial basement membrane, then promote

angiogenesis.<sup>57</sup> The significantly increased expression of MMP-2 in vehicle-treated ACLT mice was normalised with HF. TGF- $\beta$  signalling in endothelial progenitor cells can also induce angiogenesis.<sup>58</sup> We have previously shown that TGF- $\beta$  inhibition can reduce angiogenesis in subchondral bone in ACLT OA mice.<sup>26</sup> The normalisation of vessel volume and numbers in ACLT mice treated with HF was thus likely secondary to indirect suppression of MMP-2, direct inhibition of TGF- $\beta$  signalling or other additional unexplored mechanisms. We further investigated whether the increase in vasculature is from H-type vessels. H-type vessels, defined by high costaining for CD31 and endomucin (CD31<sup>hi</sup>Emcn<sup>hi</sup>), is a specific subtype of vessels that couples angiogenesis with osteogenesis.<sup>20–29</sup> Building on our prior findings that demonstrated that the formation of an ‘osteoid islet’ during OA development,<sup>26</sup> we found the increase in vasculature within the ‘osteoid islet’ was H-type vessels. H-type vessels increased after ACLT, but were equivalent to sham-operated controls when ACLT-mice were treated with HF. These results suggest that HF can attenuate OA progression by prevention of pathological angiogenesis.

The immune system has also been implicated in the pathogenesis of OA. HF has been shown to decrease nuclear factor kappa-light-chain-enhancer of activated B cells (NF- $\kappa$ B) and p38 mitogen-activated protein kinases (MAPK) in activated T cells in vitro with anticipated downstream signalling effects, such as lower interferon (INF)- $\gamma$  and tumour necrosis factor  $\alpha$  concentrations.<sup>59</sup> This may be an additional mechanism, particularly as HF has shown beneficial effects in an autoimmune arthritis mouse model.<sup>35</sup> More detailed studies are required to comprehensively understand the effects of HF on the immune system, particularly adaptive immunity.

Febrifugine has been used in Chinese herbal medicine for more than 2000 years.<sup>30–31–60</sup> The small molecule HF, a derivative of febrifugine, has been granted orphan drug status for scleroderma and Duchenne muscular dystrophy (DMD). HF has shown therapeutic promise in clinic trials for scleroderma and chronic graft-versus-host disease,<sup>32–33</sup> and is currently being investigated in effectiveness of reversing muscle fibrosis in DMD.<sup>61</sup> Our findings broaden the potential clinical application of HF. We found that HF-attenuated OA progression by targeting three subchondral bone pathological features in the early OA in rodent ACLT models. HF prevented subchondral bone changes, including reduced Th17-induced osteoclast bone resorption, reduced aberrant bone formation through inhibition of TGF- $\beta$  signalling and abrogated H-type blood vessel formation. Most importantly, articular cartilage degeneration was attenuated, suggesting that targeting of subchondral bone changes in early OA may be an effective preventive strategy.

**Correction notice** This article has been corrected since it was published Online First. The author Min Xie has been added.

**Contributors** All authors meet the International Committee of Medical Journal Editors recommendations. All authors have critically reviewed the manuscript.

**Funding** This work was supported in part by the NIH grants AR 06394 and DK 057501 (to XC).

**Competing interests** None declared.

**Provenance and peer review** Not commissioned; externally peer reviewed.

**Open Access** This is an Open Access article distributed in accordance with the Creative Commons Attribution Non Commercial (CC BY-NC 4.0) license, which permits others to distribute, remix, adapt, build upon this work non-commercially, and license their derivative works on different terms, provided the original work is properly cited and the use is non-commercial. See: <http://creativecommons.org/licenses/by-nc/4.0/>

## REFERENCES

- Brooks PM. Impact of osteoarthritis on individuals and society: how much disability? Social consequences and health economic implications. *Curr Opin Rheumatol* 2002;14:573–7.
- Lawrence RC, Felson DT, Helmick CG, et al. Estimates of the prevalence of arthritis and other rheumatic conditions in the United States: Part II. *Arthritis Rheum* 2008;58:26–35.
- Berenbaum F. Osteoarthritis year 2010 in review: pharmacological therapies. *Osteoarthritis Cartilage* 2011;19:361–5.
- Hawker GA, Mian S, Bednis K, et al. Osteoarthritis year 2010 in review: non-pharmacologic therapy. *Osteoarthritis Cartilage* 2011;19:366–74.
- van den Berg WB. Osteoarthritis year 2010 in review: pathomechanisms. *Osteoarthritis Cartilage* 2011;19:338–41.
- Kapoor M, Martel-Pelletier J, Lajeunesse D, et al. Role of proinflammatory cytokines in the pathophysiology of osteoarthritis. *Nat Rev Rheumatol* 2011;7:33–42.
- Mady H. The subchondral bone: a new frontier in articular cartilage repair. *Knee Surg Sports Traumatol Arthrosc* 2010;18:417–18.
- Goldring SR. Alterations in periarticular bone and cross talk between subchondral bone and articular cartilage in osteoarthritis. *Ther Adv Musculoskelet Dis* 2012;4:249–58.
- Roemer FW, Guermazi A, Javadi MK, et al. Change in MRI-detected subchondral bone marrow lesions is associated with cartilage loss: the MOST Study. A longitudinal multicentre study of knee osteoarthritis. *Ann Rheum Dis* 2009;68:1461–5.
- Hunter DJ, Zhang Y, Niu J, et al. Increase in bone marrow lesions associated with cartilage loss: a longitudinal magnetic resonance imaging study of knee osteoarthritis. *Ann Rheum Dis* 2006;54:1529–35.
- Raynaud JP, Martel-Pelletier J, Berthiaume MJ, et al. Correlation between bone lesion changes and cartilage volume loss in patients with osteoarthritis of the knee as assessed by quantitative magnetic resonance imaging over a 24-month period. *Ann Rheum Dis* 2008;67:683–8.
- Tanamas SK, Wluka AE, Pelletier JP, et al. Bone marrow lesions in people with knee osteoarthritis predict progression of disease and joint replacement: a longitudinal study. *Rheumatology (Oxford)* 2010;49:2413–19.
- Kothari A, Guermazi A, Chmiel JS, et al. Within-subregion relationship between bone marrow lesions and subsequent cartilage loss in knee osteoarthritis. *Arthritis Care Res* 2010;62:198–203.
- Lories RJ and Luyten FP. The bone-cartilage unit in osteoarthritis. *Nat Rev Rheumatol* 2011;7:43–9.
- Burr DB, Gallant MA. Bone remodelling in osteoarthritis. *Nat Rev Rheumatol* 2012;8:665–73.
- Layton MW, Goldstein SA, Goulet RW, et al. Examination of subchondral bone architecture in experimental osteoarthritis by microscopic computed axial tomography. *Arthritis Rheum* 1988;31:1400–5.
- Mady H, van Dijk CN, Mueller-Gerbl M. The basic science of the subchondral bone. *Knee Surg Sports Traumatol Arthrosc* 2010;18:419–33.
- Tang Y, Wu X, Lei W, et al. TGF-beta1-induced migration of bone mesenchymal stem cells couples bone resorption with formation. *Nat Med* 2009;15:757–65.
- Xian L, Wu X, Pang L, et al. Matrix IGF-1 maintains bone mass by activation of mTOR in mesenchymal stem cells. *Nat Med* 2012;18:1095–101.
- Xie H, Cui Z, Wang L, et al. PDGF-BB secreted by preosteoclasts induces angiogenesis during coupling with osteogenesis. *Nat Med* 2014;20:1270–8.
- Crane JL, Zhao L, Frye JS, et al. IGF-1 signaling is essential for differentiation of mesenchymal stem cells for peak bone mass. *Bone Res* 2013;1:186–94.
- Zhen G, Cao X. Targeting TGF $\beta$  signaling in subchondral bone and articular cartilage homeostasis. *Trends Pharmacol Sci* 2014;35:227–36.
- Khorasani MS, Diko S, Hsia AW, et al. Effect of alendronate on post-traumatic osteoarthritis induced by anterior cruciate ligament rupture in mice. *Arthritis Res Ther* 2015;17:30.
- Hayami T, Zhuo Y, Wesolowski GA, et al. Inhibition of cathepsin K reduces cartilage degeneration in the anterior cruciate ligament transection rabbit and murine models of osteoarthritis. *Bone* 2012;50:1250–9.
- Cao X. Targeting osteoclast-osteoblast communication. *Nat Med* 2011;17:1344–6.
- Zhen G, Wen C, Jia X, et al. Inhibition of TGF- $\beta$  signaling in mesenchymal stem cells of subchondral bone attenuates osteoarthritis. *Nat Med* 2013;19:704–12.
- Suri S, Gill SE, Massena de Camin S, et al. Neurovascular invasion at the osteochondral junction and in osteophytes in osteoarthritis. *Ann Rheum Dis* 2007;66:1423–8.
- Mapp PI, Walsh DA, Bowyer J, et al. Effects of a metalloproteinase inhibitor on osteochondral angiogenesis, chondropathy and pain behavior in a rat model of osteoarthritis. *Osteoarthritis Cartilage* 2010;18:593–600.
- Kusumbe AP, Ramasamy SK, Adams RH. Coupling of angiogenesis and osteogenesis by a specific vessel subtype in bone. *Nature* 2014;507:323–8.
- Pines M, Nagler A. Halofuginone: a novel antifibrotic therapy. *Gen Pharmacol* 1998;30:445–50.
- Jiang S, Zeng Q, Gettayacamin M, et al. Antimalarial activities and therapeutic properties of febrifugine analogs. *Antimicrob Agents Chemother* 2005;49:1169–76.

- 32 Gnainsky Y, Kushnirsky Z, Bilu G, *et al.* Gene expression during chemically induced liver fibrosis: effect of halofuginone on TGF- $\beta$  signaling. *Cell Tissue Res* 2007;328:153–66.
- 33 Pines M, Snyder D, Yarkoni S, *et al.* Halofuginone to treat fibrosis in chronic graft-versus-host disease and scleroderma. *Biol Blood Marrow Transplant* 2003;9:417–25.
- 34 Sundrud MS, Korolov SB, Feuerer M, *et al.* Halofuginone inhibits TH17 cell differentiation by activating the amino acid starvation response. *Science* 2009;324:1334–8.
- 35 Park MK, Park JS, Park EM, *et al.* Halofuginone ameliorates autoimmune arthritis in mice by regulating the balance between Th17 and Treg cells and inhibiting osteoclastogenesis. *Arthritis Rheumatol* 2014;66:1195–207.
- 36 Harrington LE, Hatton RD, Mangan PR, *et al.* Interleukin 17-producing CD4<sup>+</sup> effector T cells develop via a lineage distinct from the T helper type 1 and 2 lineages. *Nat Immunol* 2005;6:1123–32.
- 37 Park H, Li Z, Yang XO, *et al.* A distinct lineage of CD4 T cells regulates tissue inflammation by producing interleukin 17. *Nat Immunol* 2005;6:1133–41.
- 38 Sato K, Suematsu A, Okamoto K, *et al.* Th17 functions as an osteoclastogenic helper T cell subset that links T cell activation and bone destruction. *J Exp Med* 2006;203:2673–82.
- 39 Kotake S, Udagawa N, Takahashi N, *et al.* IL-17 in synovial fluids from patients with rheumatoid arthritis is a potent stimulator of osteoclastogenesis. *J Clin Invest* 1999;103:1345–52.
- 40 Mangan PR, Harrington LE, O'Quinn DB, *et al.* Transforming growth factor- $\beta$  induces development of the T(H)17 lineage. *Nature* 2006;441:231–4.
- 41 Bettelli E, Carrier Y, Gao W, *et al.* Reciprocal developmental pathways for the generation of pathogenic effector TH17 and regulatory T cells. *Nature* 2006;441:235–8.
- 42 Elkin M, Miao HQ, Nagler A, *et al.* Halofuginone: a potent inhibitor of critical steps in angiogenesis progression. *FASEB J* 2000;14:2477–85.
- 43 Ishii H, Tanaka H, Katoh K, *et al.* Characterization of infiltrating T cells and Th1/Th2-type cytokines in the synovium of patients with osteoarthritis. *Osteoarthritis Cartilage* 2002;10:277–81.
- 44 Shen PC, Wu CL, Jou IM, *et al.* T helper cells promote disease progression of osteoarthritis by inducing macrophage inflammatory protein-1 $\gamma$ . *Osteoarthritis Cartilage* 2011;19:728–36.
- 45 Pritzker KP, Gay S, Jimenez SA, *et al.* Osteoarthritis cartilage histopathology: grading and staging. *Osteoarthritis Cartilage* 2006;14:13–29.
- 46 Liu HP, Cao AT, Feng T, *et al.* TGF- $\beta$  converts Th1 cells into Th17 cells through stimulation of Runx1 expression. *Eur J Immunol* 2015;45:1010–18.
- 47 Gorelik L, Fields PE, Flavell RA. Cutting edge: TGF- $\beta$  inhibits Th type 2 development through inhibition of GATA-3 expression. *J Immunol* 2000;165:4773–7.
- 48 Gorelik L, Constant S, Flavell RA. Mechanism of transforming growth factor- $\beta$ -induced inhibition of T helper type 1 differentiation. *J Exp Med* 2002;195:1499–505.
- 49 Keller TL, Zocco D, Sundrud MS, *et al.* Halofuginone and other febrifugine derivatives inhibit prolyl-tRNA synthetase. *Nat Chem Biol* 2012;8:311–17.
- 50 Zhou H, Sun L, Yang XL, *et al.* ATP-directed capture of bioactive herbal-based medicine on human tRNA synthetase. *Nature* 2013;494:121–4.
- 51 Shen J, Li S, Chen D. TGF- $\beta$  signaling and the development of osteoarthritis. *Bone Res* 2014;2:14002.
- 52 Arnoldi CC, Linderholm H, Müsßbichler H. Venous engorgement and intraosseous hypertension in osteoarthritis of the hip. *J Bone Joint Surg Br* 1972;54:409–21.
- 53 Mapp PI, Avery PS, McWilliams DF, *et al.* Angiogenesis in two animal models of osteoarthritis. *Osteoarthritis Cartilage* 2008;16:61–9.
- 54 Cui Z, Xu C, Li X, *et al.* Treatment with recombinant lubricin attenuates osteoarthritis by positive feedback loop between articular cartilage and subchondral bone in ovariectomized rats. *Bone* 2015;74:37–47.
- 55 Stetler-Stevenson WG. Matrix metalloproteinases in angiogenesis: a moving target for therapeutic intervention. *J Clin Invest* 1999;103:1237–41.
- 56 Liotta LA, Tryggvason K, Garbisa S, *et al.* Partial purification and characterization of a neutral protease which cleaves type IV collagen. *Biochemistry* 1981;20:100–4.
- 57 Yurchenco PD and Schittny JC. Molecular architecture of basement membranes. *FASEB J* 1990;4:1577–90.
- 58 Cunha SI, Pietras K. ALK1 as an emerging target for antiangiogenic therapy of cancer. *Blood* 2011;117:6999–7006.
- 59 Leiba M, Cahalon L, Shimoni A, *et al.* Halofuginone inhibits NF- $\kappa$ B and p38 MAPK in activated T cells. *J Leukoc Biol* 2006;80:399–406.
- 60 Pines M, Spector I. Halofuginone—the multifaceted molecule. *Molecules* 2015;20:573–94.
- 61 McLoon LK. Focusing on fibrosis: halofuginone-induced functional improvement in the mdx mouse model of Duchenne muscular dystrophy. *Am J Physiol Heart Circ Physiol* 2008;294:H1505–7.